

Experimental test of an alignment-sensing scheme for a gravitational-wave interferometer

Nergis Mavalvala, Daniel Sigg, and David Shoemaker

An alignment-sensing scheme for all significant angular degrees of freedom of a power-recycled Michelson interferometer with Fabry-Perot cavities in the arms was tested on a tabletop interferometer. The response to misalignment of all degrees of freedom was measured at each sensor, and good agreement was found between measured and theoretical values. © 1998 Optical Society of America

OCIS codes: 220.1140, 120.3180.

1. Introduction

One of the most promising techniques for detecting gravitational waves is through the apparent change in travel time of light along orthogonal axes in the arms of a Michelson interferometer, induced by a passing gravitational wave.¹ For increasing their sensitivity, the interferometric gravitational-wave detectors currently planned for the Laser Interferometric Gravitational-Wave Observatory (LIGO)² use resonant Fabry-Perot cavities in each arm of the Michelson interferometer to increase the phase shift of the light returning to the beam splitter, as well as a partially transmitting mirror placed at the input to the interferometer to recycle the light returning toward the laser (see Fig. 1).³

In a detector with this optical configuration the two arm cavities and the recycling cavity must be resonant, and the path difference of the arms of the Michelson interferometer must result in nearly perfect destructive interference. Currently planned interferometers use extensions of a heterodyne phase-sensing technique often referred to as Pound-Drever-Hall reflection locking^{4,5} to detect longitudinal deviations from resonance. In the simplest form of this tech-

nique (applied to a simple Fabry-Perot cavity), phase-modulation sidebands outside the cavity linewidth are imposed on the incident laser light and deviations in cavity length, which detune the carrier resonance, induce an intensity modulation at the sideband frequency in reflected light proportional to length deviations that can be used in a feedback loop to keep the cavity on resonance.

An important mechanism by which the sensitivity of this resonant optical system can be degraded is angular misalignment of the interferometer mirrors with respect to the incoming laser beam. Misalignment reduces the gravitational-wave sensitivity either by allowing unwanted light power to leak out of the antisymmetric Michelson port, which increases the shot noise, or by lowering the stored light power in the arm cavities, thereby decreasing the signal induced by a gravitational wave. Consequently, for maximum gravitational-wave strain sensitivity to be achieved, the absolute angle of each mirror relative to the incoming laser beam must be less than 10^{-8} rad rms.⁶

2. Detection of Angular Misalignment

Since the modes of a misaligned resonant cavity have a different spatial profile from that of the incident beam, the spatial pattern of the fields reflected from the cavity carries information about the alignment state of the cavity. The measurement of angular misalignments in a resonant optical cavity by heterodyne detection of off-axis spatial modes was first proposed and demonstrated by Anderson and Sampas.⁷ Morrison *et al.*⁸ adapted the Pound-Drever-Hall technique by using the spatial asymmetries of the amplitude-modulated light reflected from the cavity to detect angular misalignment of the cavity mirrors with respect to the incoming laser beam. One ob-

When this study was performed, all the authors were with the Laser Interferometer Gravitational-Wave Observatory (LIGO) Project, Department of Physics and Center for Space Research, Massachusetts Institute of Technology, Cambridge, Massachusetts 02139. N. Mavalvala is now with the LIGO Project, California Institute of Technology, MS 18-34, Pasadena, California 91125. D. Sigg is now with the LIGO Project, P.O. Box 1970, MS S9-02, Richland, Washington 99352.

Received 15 May 1998; revised manuscript received 4 August 1998.

0003-6935/98/337743-04\$15.00/0

© 1998 Optical Society of America

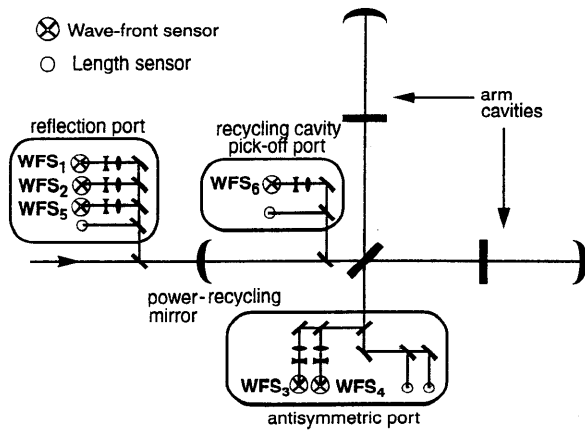


Fig. 1. Overview of the experiment. The length sensors and wave-front sensors (WFS_{*i*}) are placed at three signal detection ports. An antireflection-coated pellicle beam splitter is used to pick off a tiny fraction of the light inside the power-recycling cavity.

tains signals proportional to length deviations by detecting the total reflected light power, whereas one determines alignment signals by taking the difference of opposing halves of a split photodetector. A significant advantage of this method is that, if the cavity length is held on resonance for the carrier light frequency by use of the Pound–Drever–Hall reflection-locking technique, no additional sidebands are required to sense the deviations from perfect alignment. An important, and useful, difference between length and alignment sensing is the presence of axial or Guoy phase shifts acquired by higher-order transverse modes owing to free-space propagation.⁹ Alignment signals caused by misalignment of the input or rear mirror of the resonant cavity are thus distinguishable because of their relative phase shift.

An alignment-sensing scheme for a two-mirror resonant cavity is comprised of two quadrant photodetectors placed at specific distances from the input mirror, corresponding to the optimal Guoy phase shift for detection of input and rear mirror misalignments. The signal from each quadrant is demodulated at the modulation frequency, and the difference of two opposite pairs of quadrants is proportional to misalignment of the particular degree of freedom. Conveniently, the sum of all four quadrants gives the length-sensing signal. We refer to the quadrant photodetector and its associated electronics as a wave-front sensor. Similarly, in a complex optical system such as the power-recycled interferometer used for gravitational-wave detection, an unambiguous signal for each length and alignment degree of freedom can be obtained. Numerous signal-extraction schemes for sensing deviations from perfect longitudinal interference, based on a combination of suppressed carrier and Pound–Drever–Hall reflection-locking techniques, have been developed and tested.^{10,11} The signals for the four longitudinal degrees of freedom are sensed at one or more of three detection ports, or outputs, of the interferometer: the antisymmetric port, the reflection port, and the recycling cavity pick-off port (see Fig. 1).

Analogous to the simple cavity, alignment signals can be derived by the spatial sampling of the fields at the detection ports. Alignment signals are extracted by use of the above heterodyne phase-detection techniques; the magnitude of angular misalignments is measured by detection of the spatial gradients in the interfering carrier and sideband fields.

Distinct discriminants for ten angular degrees of freedom can be derived by judicious placement of five wave-front sensors at three detection ports. Most generally, the signal detected by the *i*th wave-front sensor is

$$\text{WFS}_i \propto \sum_j A_{ij} \Theta_j \cos(\eta_i - \eta_{ij}) \cos(\Omega_i t - \phi_{ij}), \quad (1)$$

where the sum is taken over all *j* angular degrees of freedom, Θ_j is the misalignment angle of the *j*th degree of freedom, η_i is the Guoy phase shift between the detection port and the detector, η_{ij} is the intrinsic Guoy phase shift of the signal, Ω_i is the modulation frequency, and ϕ_{ij} is the intrinsic rf phase shift of the signal. The elements of the alignment-sensitivity matrix, A_{ij} , depend on the optical parameters of the interferometer and on the particular signal-extraction scheme used. The linear approximation in Eq. (1) is good for misalignment angles, which are small compared with the divergence angle of the laser beam.

3. Experimental Test

An experimental test of these alignment techniques was performed on a tabletop scale interferometer. A schematic representation of the experiment¹² is shown in Fig. 1. The rear mirrors of the arm cavities are high reflectors, whereas the power reflectivity of each arm cavity input mirror is 0.97 and that of the power-recycling mirror is 0.92. A beam pick-off in the recycling cavity and imperfect contrast at the beam splitter introduce an additional loss of 5% in the recycling cavity, leading to a power-recycling gain of ~ 7 for the main carrier.

The laser source is a frequency- and power-stabilized Ar⁺ cw laser with a wavelength of $\lambda = 514.5$ nm and a typical output power of 250 mW. The interferometer lengths are held on resonance by use of a multiple-carrier modulation scheme.¹¹ A frequency-shifted subcarrier is generated with a double-pass acousto-optic modulator, and two pairs of phase-modulation sidebands are impressed on it with Pockels cells. A pair of phase-modulation sidebands is also impressed on the main carrier light. The carrier and sideband light is recombined by use of a beam splitter before being launched into a fiber that serves as a spatial mode filter.

The wave-front sensors consist of a quadrant photodiode with four readout channels, each of which is followed by a tuned circuit, an rf amplifier, and a mixer with low-pass filtering to achieve a low-noise downconversion of the error signal at the modulation frequency. The signals are digitized by analog-to-digital converters and read into a VME-based com-

puter system. Digital-to-analog converters are used to drive angular piezoelectric transducer actuators that tilt the interferometer mirrors about both the horizontal and vertical axes. An independently calibrated pointing system (a set of optical levers) is implemented to measure accurately the absolute tilt angles of each mirror.

Interference between a main carrier, which is resonant in the arm cavities and the recycling cavity, and a pair of phase-modulation sidebands resonant only in the recycling cavity is used to extract both length and alignment signals for the arm cavities. Differential misalignments of the arm cavity mirrors, like differential length deviations, are detected primarily at the antisymmetric port (WFS₄). Similarly, common-mode misalignments of the arm cavity mirrors are sensed at either the reflection port (WFS₅) or at the recycling cavity pick-off port (WFS₆), as are the common-mode length deviations. A frequency-shifted subcarrier and a pair of phase-modulation sidebands, all of which resonate in the recycling cavity but not in the arm cavities, are used to detect differential misalignments of the arm cavity input mirrors at the antisymmetric port (WFS₃). An additional pair of subcarrier sidebands, which is not resonant anywhere in the interferometer, is used to sense common-mode misalignments of the arm cavity input mirrors and the power-recycling mirror at the reflection port (WFS₁ and WFS₂). Since the subcarrier is antiresonant in the arm cavities, signals derived from the subcarrier and its sidebands are most sensitive to the Michelson degrees of freedom and nearly independent of arm cavity deviations. The resulting alignment-sensitivity matrix *A* is nonsingular, which makes it possible to separate individual mirror angles clearly.

The matrix elements of *A* were calculated by use of a model based on mode decomposition of the interferometer fields¹³ and inverted to give coefficients for a low-frequency (1-Hz) digital feedback system to bring the resonant interferometer into an optimal alignment state. To measure experimentally the alignment-sensitivity matrix elements, we dithered each angular degree of freedom at a distinct frequency well above the bandwidth of the angular servos; signals from the WFS's and from a set of optical levers, one for each mirror, were analyzed off-line. The Fourier transforms of the measured time series for each optical lever and each WFS were computed. By determining the signal amplitude caused by each angular degree of freedom in each WFS and optical lever spectrum and by taking into account the light power hitting the WFS's, their quantum efficiency, and their transimpedance gain, we directly calculated each element of the alignment-sensitivity matrix.

4. Results and Discussion

In Fig. 2 we plot the experimentally determined matrix elements against the values predicted by the mode decomposition model. Since the matrix elements that are predicted to be small do indeed cor-

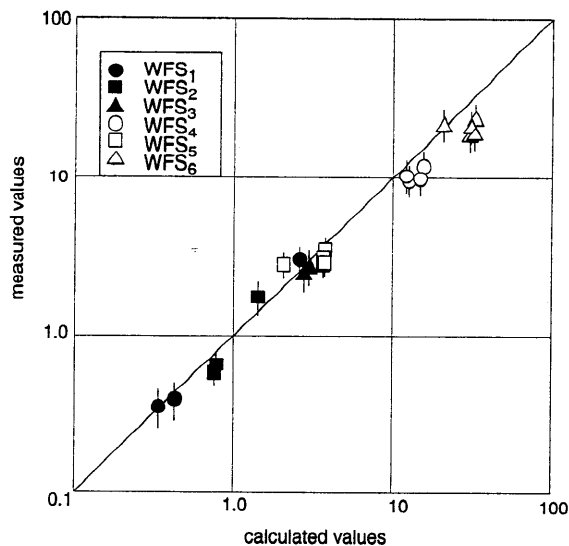


Fig. 2. Dominant elements of the alignment-sensitivity matrix compared with the values predicted by the model. Calculated values are along the horizontal axis, and the vertical axis corresponds to measured values. (All values are given in arbitrary units.) Each wave-front sensor is designated by a different symbol; the error bars are explained in the text.

respond to insignificant signals on the WFS's, only the dominant elements of the alignment-sensitivity matrix, averaged over horizontal and vertical degrees of freedom, are shown. The error bars arise from uncertainties in the power built up in the recycling cavity (6%–24%, depending on the matrix element), the Guoy phase shift in the telescopes (~1% for on-diagonal elements and 5%–20% for off-diagonal elements), the transimpedance gains of the WFS's (5%–10%), the absolute light power incident on each detector (6%), the modulation indices (5%–10%), and the calibration of the pointing system (10%). The statistical uncertainties are small, typically below 3%. Since these uncertainties are independent of each other, they are added in quadrature, resulting in approximately $\pm 20\%$ total uncertainty for the matrix elements plotted in Fig. 2.

The quantitative agreement between the modal model predictions and the measurement, evidenced in Fig. 2, is a strong validation of the model. It gives us confidence that a complete set of alignment signals can be experimentally determined in a complex resonant optical system with sufficient precision to enable a precision alignment sensor. Based on the wave-front-sensing scheme, we have designed an automatic alignment system for the LIGO.⁶ For the alignment effects to be kept from deteriorating the gravitational-wave design sensitivity by more than 1%, some of the angular degrees of freedom have to be controlled within 10^{-8} rad rms.⁶ The projected shot-noise-limited sensitivity for the LIGO WFS's is between 10^{-15} and 10^{-13} rad/ $\sqrt{\text{Hz}}$ (see Table 3 of Ref. 6). Thus for a servo system with a typical bandwidth of a few hertz the sensing noise is orders of magnitudes below the required alignment tolerance.

We conclude that the wave-front-sensing technique is well understood, both theoretically and experimentally, and that this technique is feasible for closed-loop servo control of complex resonant optical interferometers.

We thank our colleagues on the LIGO project who helped us carry out this experiment and gave us many useful suggestions and comments, particularly R. Weiss and S. Whitcomb. Most of all, we thank Y. Hefetz, who initiated this experiment and much of the analysis preceding it. This study is supported by National Science Foundation grant PHY-9210038. D. Sigg was partially supported by the Swiss National Science Foundation.

References and Note

1. R. Weiss, "Electromagnetically coupled broadband gravitational antenna," MIT Res. Lab. Electron. Q. Prog. Rep. **105**, 54-76 (1972).
2. A. Abramovici, W. E. Althouse, R. W. P. Drever, Y. Gürsel, S. Kawamura, F. J. Raab, D. Shoemaker, L. Sievers, R. E. Spero, K. S. Thorne, R. E. Vogt, R. Weiss, S. E. Whitcomb, and M. E. Zucker, "LIGO: the Laser Interferometer Gravitational-wave Observatory," *Science* **256**, 325-333 (1992).
3. See, for example, R. W. P. Drever, "Interferometric detectors for gravitational radiation," in *Gravitational Radiation*, N. Deruelle and T. Piran, eds. (North-Holland, Dordrecht, The Netherlands, 1983), pp. 321-338.
4. A. Schenzle, R. DeVoe, and G. Brewer, "Phase-modulation laser spectroscopy," *Phys. Rev. A* **25**, 2606-2621 (1982).
5. R. W. P. Drever, J. L. Hall, F. V. Kowalski, J. Hough, G. M. Ford, A. J. Munley, and H. Ward, "Laser phase and frequency stabilization using an optical resonator," *Appl. Phys. B* **31**, 97-105 (1983).
6. P. Fritschel, N. Mavalvala, D. Shoemaker, D. Sigg, M. Zucker, and G. González, "Alignment of an interferometric gravitational wave detector," *Appl. Opt.* **37**, 6734-6747 (1998).
7. D. Z. Anderson, "Alignment of resonant optical cavities," *Appl. Opt.* **23**, 2944-2949 (1984); N. Sampas and D. Z. Anderson, "Stabilization of laser beam alignment to an optical resonator by heterodyne detection of off-axis modes," *Appl. Opt.* **29**, 394-403 (1990).
8. E. Morrison, B. J. Meers, D. I. Robertson, and H. Ward, "Experimental demonstration of an automatic alignment system for optical interferometers," *Appl. Opt.* **33**, 5037-5040 (1994); E. Morrison, B. J. Meers, D. I. Robertson, and H. Ward, "Automatic alignment of optical interferometers," *Appl. Opt.* **33**, 5041-5049 (1994).
9. A. E. Siegman, *Lasers* (University Science, California, 1986) pp. 682-685.
10. M. W. Regehr, F. J. Raab, and S. E. Whitcomb, "Demonstration of a power-recycled Michelson interferometer with Fabry-Perot arms by frontal modulation," *Opt. Lett.* **20**, 1507-1509 (1995).
11. D. Sigg, N. Mavalvala, J. Giaime, P. Fritschel, and D. Shoemaker, "Signal extraction in a power-recycled Michelson interferometer with Fabry-Perot arm cavities by use of multiple-carrier frontal modulation scheme," *Appl. Opt.* **37**, 5687-5693 (1998).
12. N. Mavalvala, "Alignment issues in laser interferometric gravitational-wave detectors," Ph.D. dissertation (Massachusetts Institute of Technology, Cambridge, Mass., 1997).
13. Y. Hefetz, N. Mavalvala, and D. Sigg, "Principles of calculating alignment signals in complex resonant optical interferometers," *J. Opt. Soc. Am. B* **14**, 1597-1605 (1997).